

LOGISTICS MOTION ASSIGNMENTS IN ROBOTIZED SYSTEMS

NAQIB DANESHJO¹, MILAN MAJERNIK¹
MARIAN KRÁLIK², ENAYAT DANISHJOO³

¹University of Economics in Bratislava
Faculty of Business Economics with seat in Kosice
Kosice, Slovak Republic

²Slovak Technical University in Bratislava
Faculty of mechanical engineering
Bratislava, Slovak Republic

³Thk rhythm automotive GMBH
Duesseldorf, Germany

DOI: 10.17973/MMSJ.2017_02_2016193

e-mail: daneshjo47@gmail.com

The authors within the scientific contribution present the optimization of the trajectory of an industrial robot in selected systems. The thesis deal with the task of creating collision-free trajectories of industrial robots, based on the geometric information describing the configuration space with respect to the possibility of robot kinematic. There are introduced the basic methods of exact and probabilistic motion planning. Loading, processing and parameterization of 3D objects. Using algorithms for testing of collisions and visibility. Design of the basic trajectory, which is later optimized to achieve the minimum distance traveled between origin and destination point of travel.

KEYWORDS

robot, logistics, trajectory planning, collision free trajectory, off-line programming

1 INTRODUCTION

Elasticity and flexibility entail a change in the methods of the proposal of each structural unit and application. In its initial phase, the proposal of technical equipment by means of the elements of fixed automation was already prepared with regard to the optimization of individual motion, minimizing the amount of the actuators, linear guides, rotary joints, tappets and the like. In contrast, the proposal of robotised station involves co-operation of multiple divisions with different impact on the final proposal of the device. A balanced link between the spatial arrangement, the technological requirements, the control system, the choice of communication protocols, justification for the financial costs, time availability of the components and a lot of other requirements led to the final nature of the device. The cooperation of a multidisciplinary team at different time stages of the project implementation gives rise to the sufficient space for the further optimization of the device throughout its life cycle.

Successful addressing of the issue of the trajectories optimization of the industrial robots will have a positive impact on the increase in the productivity of new or already implemented applications. The significance of the impact of the trajectory optimization will grow with the increasing rate of the motion assignments compared with the rate of the technological activities of a robot [Králík 2013], [Daneshjo 2015].

2 THE OPTIMIZATION OF THE TRAJECTORY OF THE INDUSTRIAL ROBOTS (IR)

Based on the mentioned findings, individual areas were processed into the separate functional units in the form of the code of the programming languages, c++, OpenGL and OpenMP, so as they created a program containing the opportunity of parameterization of the input values for computation of the trajectory of IR. Meanwhile, these enabled its

optimization by changing the input data and, finally, they enabled to visualize the modelled scenarios by means of verifying the results of the calculation. The steps for creating the trajectory of the IR can briefly be summarised into the following points:

1. Importing the geometry of all the objects.
2. Optimization of the number of triangles for the selected objects if necessary.
3. Generating the default and target points of the trajectory of IR.
4. Generating set (diagram) of transition points by the Probabilistic Road Map (PRM)
5. Computation of the matrix of distance D between points.
6. Computation of the matrix of visibility Ψ between points.
7. Determination of the transition points from the logical product of matrix of distance and visibility.
8. Generating the matrix G_{PRM} for the diagram of the transition edges.
9. Computation of the distance between points.
10. Determination of the shortest distance of the transition edges between the default and target points.
11. Generating a set of new points by the PRM for each point in step 9.
12. Repetition of steps 5 to 9 for new points.
13. Generating a trajectory of an IR based on the found points connecting the start and finish by the shortest distance.
14. Distribution of the trajectories into smaller segments.
15. Collision testing between an IR and an obstacle/barrier by-passing the segments of the generated trajectory
16. In the case of collision, the transition edge will be excluded from the matrix of visibility.
17. Repeating steps 13 to 16 until a collision-free trajectory is found or the assessed position of the target point is unavailable.

2.1 THE PLANNING PHASE OF THE TRAJECTORY – THE DIAGRAM OF THE PRM POINTS

The degree of probability is mainly affected by the parametrization and the way of generation the points. The properties of the diagram together with reliability of the PRM methods can be affected by various parameters:

- Placement of the points
- The size of the space in which the diagram was created
- The number of the points
- Location of the diagram

Fig. 1 shows randomly generated placement of the points in the plane and in the space. In the case of mobile robot navigation, points in the

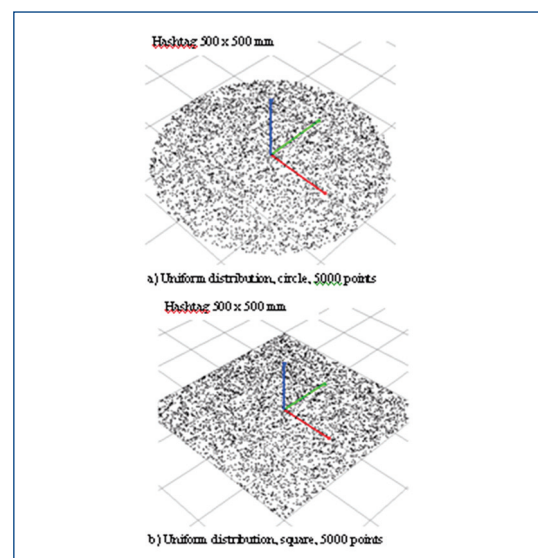


Figure 1. The points of the 3D PRM diagram bounded by a circle and a rectangular

plane or copying the terrain at a constant distance in the direction of the coordinate Z would be used. In order to calculate the trajectory of IR, it is necessary to generate points in the space. Points may be spread uniformly or by means of some of the known distribution characteristics such as the Gaussian, the Laplace arcsine, and the like [Szakall 2002], [Nagy 1987].

The number of points should reflect the size of the boundaries in which the motion assignment will be dealt with and the geometry of the obstacles so as to cover the narrow areas in which it is necessary to divide the trajectory into shorter segments. The number of points also has an impact on the computational time, whereas too many points can result in the disproportionate extension. The complexity is expressed by $O\{n^2\}$, where n is the number of points. Properly chosen location diagram can minimize the number of points [Szakall 2003].

2.2 MATRIX OF THE PLACEMENT OF POINTS OF THE DIAGRAM

The computations of the distance between the points and determination of the maximum value Δ were set as one of the optimization parameters. Excluding the points whose spacing was greater than the specified criterion significantly accelerated the calculation process in all other phases by eliminating the formation of the transition edges between overly distant points, which would not likely contribute to solving the assignment. The computations and determination of values of the individual members of the matrix are presented in equations 1 and 2. Storing the numerical values of distances generated large amounts of data, so the matrix was designed to save and store only the values of the test results in the range of *true* or *false*

$$d_{mn} = \sqrt{(x_m - x_n)^2 + (y_m - y_n)^2 + (z_m - z_n)^2} \quad (1)$$

$$D = \begin{bmatrix} n_{11} & \dots & n_{1n} \\ \vdots & \ddots & \vdots \\ n_{m1} & \dots & n_{mn} \end{bmatrix} \quad (2)$$

for $m = n$ equals the number of transition points
 If $d_{mn} \leq \Delta$ then $n_{mn} = true$,
 for all $m = n$ the value will be $n_{mn} = false$.

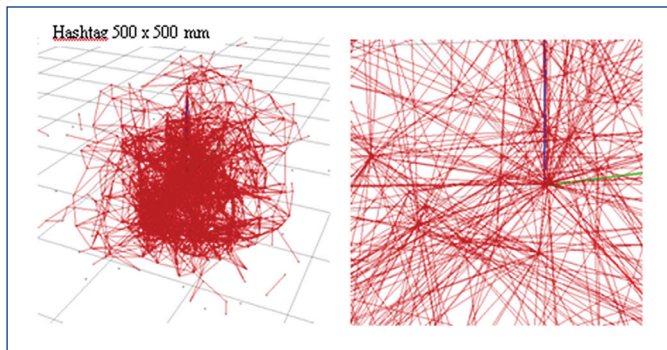


Figure 2. Transition edges restrained by maximum spacing between points

Adding the distance matrix to the calculation enabled us to generate denser point mesh at the same computational time.

2.3 MATRIX OF VISIBILITY OF THE POINTS OF THE DIAGRAM

The transition edges were formed by a line bounded by two points of the diagram. Visibility between the points algorithm was commutated by algorithm for calculation of the collision between the line and triangular surfaces of the objects. The algorithm in [1] was used to solve the assignment. The visibility test was only conducted on the edges of the diagram meeting the condition of the maximum distance in the matrix D . The other edges were directly identified as impassable [Szakall 2003].

$$\psi = \begin{bmatrix} n_{11} & \dots & n_{1n} \\ \vdots & \ddots & \vdots \\ n_{m1} & \dots & n_{mn} \end{bmatrix} \quad (3)$$

for $m = n$ equals the number of the transition points

If the test result of the collision is negative, then the value is expressed as $n_{mn} = true$, and it expresses the availability of the edge for calculation of the trajectory. The collision test had to be conducted for each transition edge and every surface of the test object. The number of tests grows exponentially with the number of points and the complexity of the subject. The complexity of the test is $O\{n^2m\}$ where n is the number of points between which it is possible to establish a link without colliding with the test object and m is the number of surfaces of the object. Table 1 lists the times of the visibility computations for the various configurations of the maximum distance and point restriction [Szakall 2005], [Pires 2007].

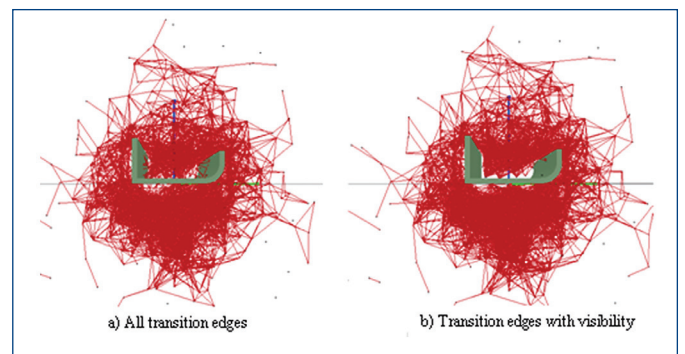


Figure 3. Generation of the transition edges in the phase of visibility testing

The collision test of a line and triangular face – The Visibility solution							
Input: Object A The number of triangular surfaces for each object: 824 Even distribution of points in the volume of a sphere of diameter $d = 2000$ mm							
Output: The collision of a line and triangular surface, <i>true/false</i> Computational time The number of transition edges							
No.	Max. distance The number of points	2000 mm time [s]	1500 mm time [s]	1000 mm time [s]	500 mm time [s]	250 mm time [s]	100 mm time [s]
1	512 The number of transition edges:	1,322 (142203)	1,171 (132295)	0,615 (76636)	0,156 (16596)	0,047 (2686)	0,002 (195)
2	1024 The number of transition edges:	5,008 (576006)	4,438 (535282)	2,298 (309856)	0,446 (66579)	0,097 (10658)	0,008 (777)
3	2048 The number of transition edges:	19,457 (2281049)	17,378 (2116294)	8,881 (1228038)	1,912 (263308)	0,321 (41861)	0,030 (3087)
4	4096 The number of transition edges:	75,961 (9274340)	66,684 (8621779)	36,217 (5017909)	6,667 (1082241)	1,135 (170089)	0,117 (12355)
5	8192 The number of transition edges:	304,463 (37208403)	275,251 (34633826)	142,548 (20283482)	26,454 (4375846)	4,146 (685996)	0,386 (49104)

Table 1. Mesh of the transition edges for various parameters

Visualization of the highlighted configurations presented in Table 1 is shown in Fig. 4. The distribution of transition edges clearly indicates that isolated clusters of connections were formed in alternative a). The sufficient number of passages was not created even if there was a case of an absent obstacle/barrier in the configuration space of the IR. There was secured a link of the space in alternative b), but there was not generated the sufficient number of links in order to create an effective trajectory in the area of the barrier/obstacle boundaries. The average distance of the points approached the maximum distance restraint in alternative c). A sufficient number of points were generated to pass by a simple obstacle/barrier.

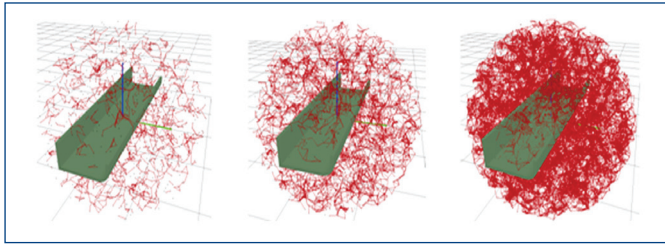


Figure 4. Mesh of the transition edges for different parameters

The logical product of the two matrices results in an optimized matrix of the usable transition edges.

$$G_{PRM} = D \wedge \psi \quad (4)$$

Summarizing the knowledge of the method of establishing the PRM diagram, matrix of the distance and visibility can be expressed by the following evaluation:

- Restraining the maximum distance significantly reduces the computational time required; it is also necessary to choose a value with a view to the shape and geometry of the obstacles/barriers so as the narrow areas with difficult accessibility and the geometry of the end effector.
- It is necessary to properly select the point distribution and minimize the space volume in which the points are generated.
- For an even distribution of the points, there must be a restraint for distances greater than the average distance of the points.
- The Gaussian distribution is suitable for the local points adding to the diagram, for example in the spot welding of the fixture.

3 GENERATION OF THE TRAJECTORY

The segments created by the transition edges form a diagram, respectively the mesh from which the path between any two points can be generated. It is necessary to determine the default and target points in the diagram to generate the trajectory. To calculate the shortest distance between two points, the Dijkstra algorithm was used.

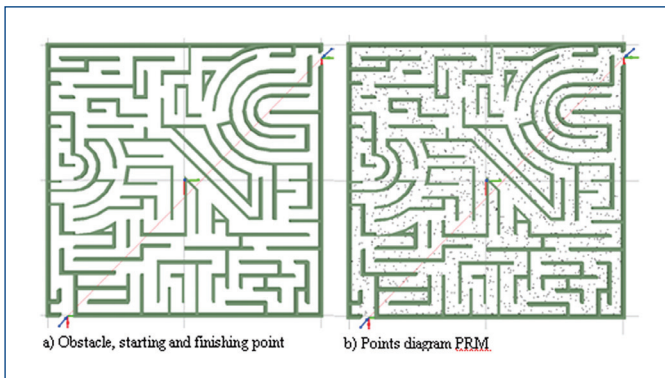


Figure 5. Generation of the trajectory by PRM

The algorithm saves all the node in the priority row classified by the distance from the source. The default point reached the value of 0 in the first iteration and all other points reach the infinite distance. The algorithm selected a node with the shortest distance at each step and it was, then, classified within the processed nodes. Next, it went through all previously unprocessed children and they were added to the queue if it had not been included yet. It verified whether the distance was shorter than it was before it was included in the process. For all children, the validity of equation 5 was verified. If the inequality applied, a new distance was set for the child and a processed node was set as its predecessor. After passing all the descendants, the node with the shortest distance was selected and the cycle repeated. The algorithm terminated after going through all nodes.

$$\text{Distance}_{\text{processed}} + d_{\text{processe/child}} < \text{Distance}_{\text{childe}} \quad (5)$$

Generation of the trajectory was designed with a view to the versatility of its use and can be applied for example in navigation of mobile robots in a familiar environment. Fig. 5 shows the process of finding the shortest trajectory in a maze and it shows the main steps taken by means of the method PRM at the same time. The shape and length of the trajectory affected the number of points of the diagram. Table 2 shows the results of the experiment with a different number of points.

Calculation of collision-free trajectory					
Input: Object B The number of triangular surfaces forming a maze: 2104 Even distribution of points in a square, the dimensions: 1000 mm x 1000 mm Path Width: 40 mm					
Output: Trajectory Length of trajectory Computational time Number of segments					
No.	Parameter Number of points	Length of trajectory [mm]	Number of segments [-]	Computational time [s]	Number of edges [-]
1	452	2603.1347	19	2.449	2654
2	904	2274.5722	22	9.048	10746
3	1356	2189.1418	19	19.906	23782
4	1808	2098.1262	22	35.755	41228
5	2260	2063.8686	23	55.052	64538
6	2712	2057.4982	23	79.435	93490
7	3164	2043.2020	24	107.718	128206
8	3616	2013.8559	25	143.084	169114
9	4068	2009.6892	24	178.246	214760
10	4520	2005.0350	27	217.184	264086
11	4972	1997.5869	25	262.237	316984
12	5424	1969.7418	24	315.479	379978
13	5876	1966.7296	25	370.549	441784
14	6328	1966.5820	25	428.612	518268
15	6780	1950.2268	25	491.558	593678

Table 2. The length of trajectory as a function of the number of points

The interpretation of the relationship between the width of a narrow place of trajectories, the width of the path and the number of the generated points in Diagram 3 in this case. The diagram shows the number of generated points to the width of the path in accordance with equation 6.

$$P_{PRM} = \frac{S}{\sqrt{D/Q}} \quad (6)$$

- S – the width of a narrow place,
- D – total area,
- Q – the number of points

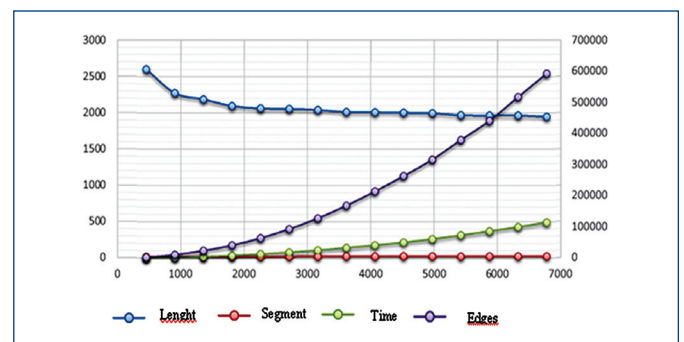


Figure 6. Generation of the trajectory by PRM

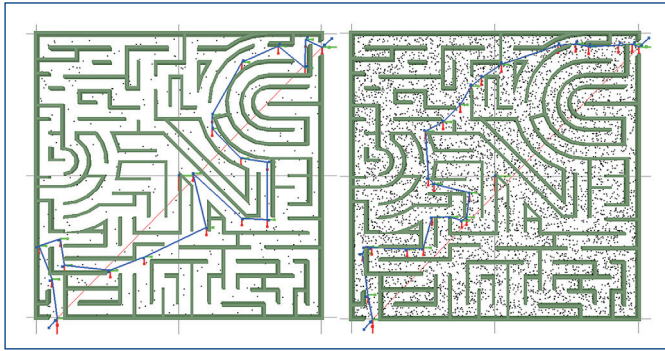


Figure 7. Display of the longest and shortest trajectories

3.1 THE EVALUATION OF THE EXPERIMENT RESULTS

The results can be interpreted in the following way:

- The impact on the length of the trajectory decreases after it has reached the density of the two points to the width of the narrow place.
- In the case of generation of points in the space for the volume of a sphere of a diameter of 1000 m, it was necessary to generate around 46,800 points to achieve the same density.

Table 2 shows that the calculation of the indicated number of points is not feasible by means of the common computer technology and, therefore, it is necessary to propose solution optimization [Szakall 2005], [Daneshjo 2014].

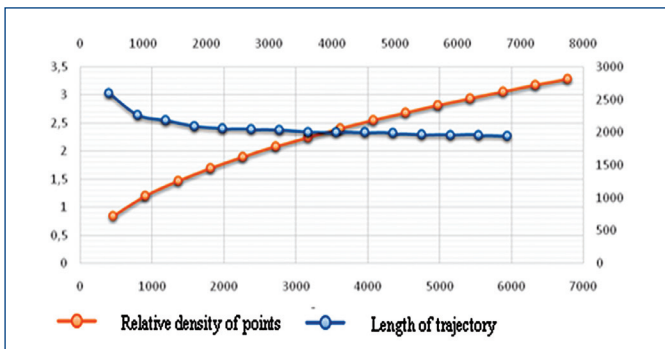


Figure 8. Relative density of points to the size of the narrow place

3.2 EXTENSION OF THE METHODOLOGY OF TRAJECTORY GENERATION

The previous experiments clearly indicated that generation of a sufficient number of transition points in the entire configuration space of IR was not effective. It was necessary to propose a solution that would reduce the number of points and would not have a significant impact on the calculation of the trajectory at the same time. As a possible solution to this issue appeared to be extending the methodology of point generating into two phases:

- Generation of the low density points in the first phase,
- Creating an approximate trajectory based on the diagram consisting of segments n ,
- Removal of the original points of the diagram,
- Creating new points in the local environment for each segment,
- Repetition of the steps for generation of the matrix of distance and visibility of the newly established set of points.

Gradual extension of the methodology is shown in Fig. 9. The example included the spot welding preparation process of the left trace consisting of 103632 triangular surfaces. In the first phase, 1568 pixels of diameter of 2200 mm were generated. A preliminary trajectory

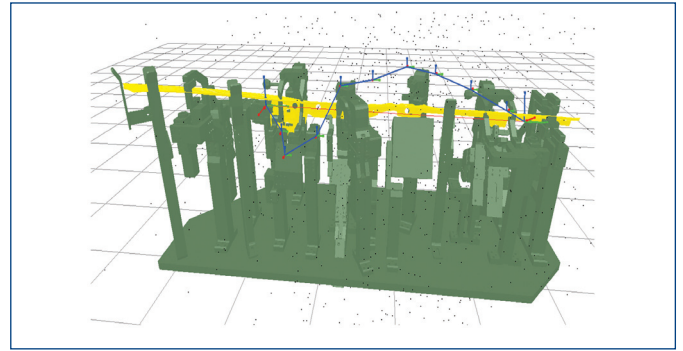


Figure 9. Welding preparation process, Skoda Fabia, left trace

consisting of 10 segments was generated using the mentioned pixels. Generation of the trajectory took 9 seconds. The second stage consisted of generating a new set of points of a diameter of 700 mm at the beginning of segments and in the target point. To highlight the method a denser mesh of 17248 points was generated [Kuffer 2000].

4 EVALUATION OF THE EXPERIMENT RESULTS

Before the first phase was launched, an approximate trajectory, which could be done between the default and target points by the IR, was not known. Moreover, it was necessary to cover a large part of the work area by means of the PRM diagram. The use of information obtained by the approximate calculation of the first phase allowed more accurate applying of the points distribution in the predicted area of the resulting trajectory.

Creating the trajectory, which was conducted in the previous part, was only the first stage of the process. The trajectory needed to be tested along the entire length for the collision occurrence between the peripheral areas and the robot including the end effector. To test the algorithms of generation and optimization of the trajectory, an assembly of spot welding of the Skoda Fabia 2015 trace was selected. The placement of the trace parts is in the preparation plant in Fig. 9. List of individual objects is shown in Table 3.

Configuration of the objects				
No.	Object	Size [kB]	Number of surfaces [-]	
1	The base of the robot- „BASE.stl“	2160	7920	
2	Axis 1 - „LINK01.stl“	1961	7192	
3	Axis 2 - „LINK02.stl“	974	3572	
3	Axis 3 - „LINK03.stl“	1277	4680	
4	Axis 4 - „LINK04.stl“	1508	5530	
5	Axis 5 - „LINK05.stl“	580	2124	
6	Axis 6 - „LINK06.stl“	391	1434	
7	Welding pincers- „V136517000B-00.stl“	4 328	15874	
8	Welding preparation- „SPS13-017.stl“	27 459	100714	
9	Assembly of the trace- „6V6.809.401-402_17_7_2013.stl“	4 570	16770	
The position of the default and target points of IR				
No.	Name	XYZ [mm]	Direction Smer Z [mm]	Rotation Z [rad]
11	p10	1901.14, 1000.06, 1020.0	-0.500, 0.000, 1.000	-1.57
2	p20	1982.20, -138.40, 1065.4	-0.100, 0.000, 1.000	1.57

Table 3. The objects of the test department

The trajectory was created by gradual passing of edges of the diagram by the robot and testing to learn whether a collision with the welding plant or the welded part occurred during moving along the edge. If a collision occurs, the edge will be marked as impassable and excluded from the further tests. Labelling the impassability of the edge led to selecting second shortest trajectory that could be created from the available data in the next iterations of the Dijkstra algorithm.

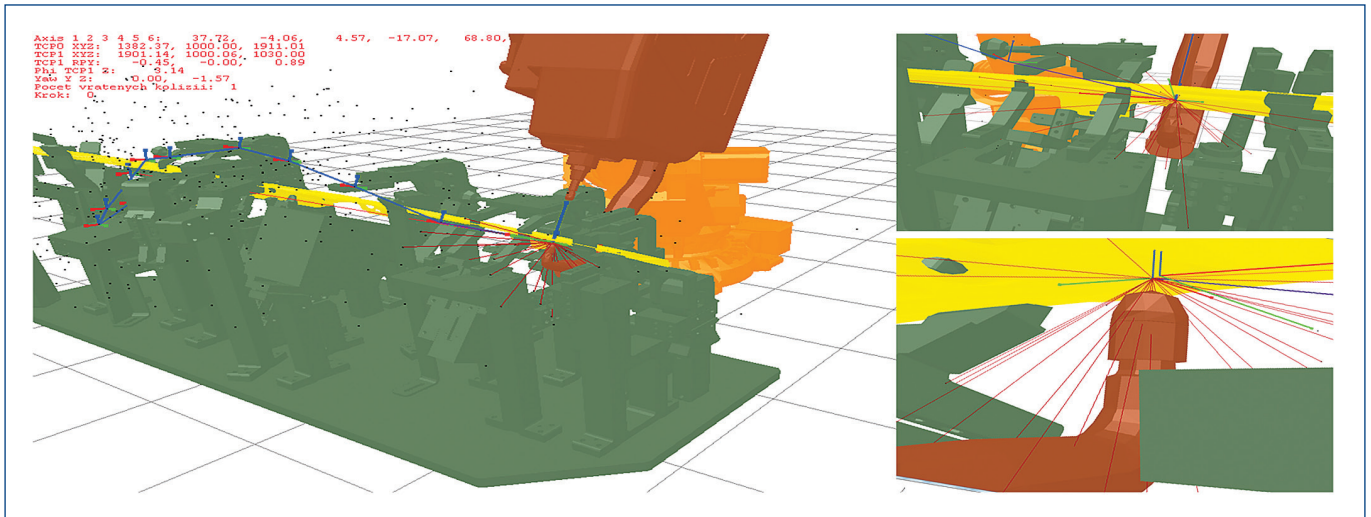


Figure 10. The segments of the trajectory in the default point

The visualization in Fig. 10 shows that the edges were only generated in the lower part and they were placed below the part whose geometry prevented the generation of the edges upwards at the same time. This situation was achieved by deliberate moving of the default point towards the direction below the part. If the exact position of the point indicated in the drawings was placed in the thickness of the welded metal sheet, transition edge would not be created. The opposite case occurred when the position of the point was below the part. In that case, all the edges were generated upwards in terms of visibility. Hence, this always causes a collision between the arms of the pincers and the plant due to the structure of the C-shaped welding pincers. Solving this geometry inaccuracy, which may occur during setting the location in relation to the part and TCP, was exclusion of the visibility test for the default and target points as shown in Fig. 11. Moreover, it was necessary to conduct the collision tests that removed the unusable edges. On one hand, the modification slightly prolonged the computational time by progressive removal of the edges during the collision test. On the other hand, the situation in which it was not possible to generate the edges in the appropriate position, did not occur [Hsu 2005].

5 THE TRAJECTORY OF THE IR

In order to verify the proposed solution with regard to the maximum level of algorithms usability in various applications, spot welding application was chosen to take part in testing. Compared with the manipulation applications, the trajectories were generally more complex with a lot of reorientations of the tool in the three axes of the TCP. At the same time, the configuration space contained IR narrow places created by clamping brackets of the preparation plant and geometry of the welded

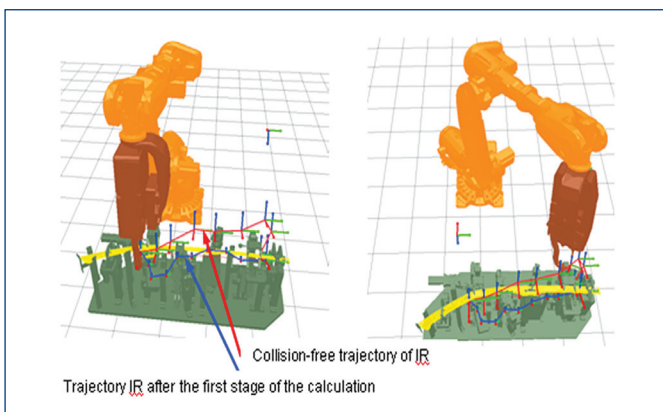


Figure 11. The final trajectory of IR

part. By-passing of the obstacles/barrier is a relatively complicated task in terms of the available computational time, whereas the decision between the change of the re-orientation of the tool or maintaining its original orientation and only changing the position can have both, negative and positive impact on the result. If the trajectory is composed of several tens to hundreds of short segments, information processing on the rotation of the end effector presents large computational complexity [Szakall 2005].

It should be emphasized that any restraint during testing of the available configurations of the rotation of the IR leads to deteriorating the optimization results. In the worst-case scenario, it increases the likelihood of not finding a collision-free trajectory between the given points. Determination of the extent of re-orientation in the individual axes while moving through the trajectory segments is one of the points in the framework of future solutions.

Evaluation of experiment results:

- The results in Table 4 can be interpreted as follows:
- Creation of 600 points, that is 60 for each segment generated in the first stage, was not sufficient to calculate the collision-free trajectory resulting in not finding the path between the default and target points,
- Due to the random placement of the generated points in the space, an increase in their number (to some extent) does not necessarily lead to finding a shorter trajectory,
- Following the experiment described in chapter 6.1.4, in which the points on the two-dimensional surface with significantly greater density were generated and their number for every further step doubled, it would be necessary to generate a substantially greater number for the optimization of the trajectory in the space,
- The time required for calculation increases significantly with the increasing number of steps for finding a path. Collisions testing has a major impact on the speed of computation.

6 CONCLUSIONS

In terms of achieving the objectives, the solution analysis with regard to obtaining the sufficient knowledge on the kinematic properties of IR was conducted. Solving the inverse kinematics showed the ambiguity of the end effector position computation; this should have been considered during computing the trajectory and its visualization. The classic approach of calculating collisions, chapter 4.3, was fully functional, but the results of the experimental part clearly indicated that the computation consisted of a narrow place and it was time consuming even after the optimization of the performance of the CPU had been done. Due to the computational complexity, the proposal of the optimization criteria was narrowed down to determination of the shortest trajectory done by an IR

along the path consisting of segments connecting the limited number of transition edges. The optimization criteria were rather used to determine the appropriate range of parameters so as to achieve the results of the computations in an acceptable period of time.

The proposal of the planning algorithms led to the successful computation of collision-free trajectory done by an IR. The solution was verified by the models of actual spot welding applications, so that the simulation approached actual conditions as closely as possible. The growing number of IRS in the industry and the private sector will require finding a new way to the contemporary complex way of programming the assignments for robots. It will be necessary to create more advanced 90 programming language. This way the robot will be fed with the more complex assignments by a single order unlike under the current conditions when the robot must be programmed for each individual motion and processing of each logic instruction separately. Improvement, development and amendments of the proposed algorithms can be divided into three main areas. The first one focuses on increasing probability of finding the trajectory by the PRM method and adding new procedures to the configuration browser of an IR.

ACKNOWLEDGMENTS

This paper was written in frame of the work on the projects VEGA 1/0936/15

REFERENCES

- [Daneshjo 2014] Daneshjo N. Localization of logistics objects. In: The 17th International Scientific Conference Trends and Innovative Approaches in Business Processes, 19. 12. 2014, Kosice – SĽF, TUKE – ISBN 978-80-553-1864-6,
- [Daneshjo 2015] Daneshjo, N., – Samer A., A. Localization of logistics objects. In: Interdisciplinarity in theory and practice – Journal for Presentation of Interdisciplinary Approaches in Various Fields – ITPB, Arad – Romania: Nr.:8, p. 187-192, ISSN: 2344-2409 , ISSN-L: 2344 – 2409
- [Hsu 2005] Hsu, D., – Latombe J.C. – Kurniawati H.: On the Probabilistic Foundations of Probabilistic Roadmap Planning. International Journal of Robotics Research, San Francisco, CA,
- [Kralik 2013] Kralik, M., et al. Surface layer hardening. In: Scientific Proceedings Faculty of Mechanical Engineering 2013, Bratislava: STU., pp. 107-112.
- [Kuffer 2000] Kuffner, J. J., – Lavelle, S. M. RRT-Connect: An Efficient Approach to Single-Query Path Planning Proceedings of the IEEE International Conference on Robotics & Automation, San Francisco, CA, p. 995-1001,
- [Nagy 1987] Nagy, F – Siegler A.: Engineering Foundations of Robotics. Prentice – Hall International (UK) Ltd, London, ISBN 0-13-278805-5.
- [Pires 2007] Pires, J. Industrial Robots Programming: Building Applications for The Factories of The Future, Springer: University of Coimbra, ISBN 0-387-23325-3.
- [Szakal 2002] Szakall, P. Robotics – Trend 3rd millennium, ABB Spektrum. year IV, No. 4,
- [Szakal 2003] Szakall, P. Optimization robotized workplace, AT&P Journal No. 09, p. 34-35
- [Szakal 2005] Szakall, P. Industrial robots in manipulation applications, ABB Spektrum, year VII, No. 2,

CONTACTS

Assoc. prof. Naqib Daneshjo, PhD.
University of Economics in Bratislava
Faculty of Business Economics with seat in Kosice
Department of Commercial Business
Tajovskeho 13, 041 30 Kosice, Slovak Republic
tel.: 00421 55 722 3248, e-mail: daneshjo47@gmail.com
www.euke.sk

prof. h. c. prof. Ing. Milan Majernik, PhD.
University of Economics in Bratislava
Faculty of Business Economics with seat in Kosice
Department of Management
Tajovskeho 13, 041 30 Kosice, Slovak Republic
tel.: 00421 55 722 3258, e-mail: milan.majernik@euke.sk,
www.euke.sk

Assoc. prof. Marian Kralik, PhD.
Slovak Technical University in Bratislava
Faculty of mechanical engineering
Institute of manufacturing systems, environmental technology
and quality management
Nam. slobody 17, 812 31 Bratislava, Slovak Republic
tel.: 00421 02 572 96579, e-mail: marian.kralik@stuba.sk,
www.sjf.stuba.sk

Ing. Enayat Danishjoo, PhD.
Thk rhythm automotive GMBH
Fichtenstraße 37, 40233 Düsseldorf, Germany
Nám. slobody 17, 812 31 Bratislava, Slovak republic
tel.: 0049 162 8547669
e-mail: danishjoo@web.de